



# Seismic Performance Management of Aging Road Facilities in Korea: Part 2 – Decision-making Support Technology and Its Application

Dongjoo Kim<sup>1a</sup>, Junho Song<sup>2b</sup>, Young-Joo Lee<sup>3c</sup>, Sungsik Yoon<sup>4d</sup>, Dong Keun Yoon<sup>5e</sup>,  
Yong Kang Lee<sup>6f</sup>, Youngjun Kwon<sup>7b</sup>, Dongkyu Lee<sup>8g</sup>, and Yeon-Woo Choi<sup>9h</sup>

<sup>a</sup>Member, Korea Authority of Land & Infrastructure Safety, Jinju 52856, Korea

<sup>b</sup>Member, Dept. of Civil and Environmental Engineering, Seoul National University, Seoul 08826, Korea

<sup>c</sup>Member, Dept. of Urban and Environmental Engineering, Ulsan National Institute of Science and Technology, Ulsan 44919, Korea

<sup>d</sup>Dept. of Artificial Intelligence, Hannam University, Daejeon 34430, Korea

<sup>e</sup>Dept. of Urban Planning and Engineering, Yonsei University, Seoul 03722, Korea

<sup>f</sup>Korea Authority of Land & Infrastructure Safety, Jinju 52856, Korea

<sup>g</sup>Dept. of Civil and Environmental Engineering, Seoul National University, Seoul 08826, Korea

<sup>h</sup>Member, Dept. of Urban Planning and Engineering, Yonsei University, Seoul 03722, Korea

## ARTICLE HISTORY

Received 11 April 2023  
Accepted 11 October 2023  
Published Online 6 December 2023

## KEYWORDS

Seismic performance  
Road facilities  
Aging  
Fragility curve  
Limit states

## ABSTRACT

This study aims to develop a decision-making support system for managing aged road facilities in a target road network based on seismic performance evaluation. For this purpose, the seismic fragility considering aging effect is analyzed for bridges, tunnels, retaining walls, and slopes to assess the direct damage to individual road facilities, as described in the companion paper. In this paper, based on the seismic fragilities of road facilities, the degradation of the road network's seismic performance and social and economic resilience is evaluated. The decision support system is then developed based on the seismic risk assessment method (SRA) for the seismic management of old road facilities suitable for domestic conditions. The SRA method includes the calculation of direct and indirect damage of road networks, the assessment of socio-economic resilience to disaster in South Korea, and the basis for decision-making. In addition, a geospatial information-based software for repair and reinforcement decisions is developed. The developed decision-making support software is verified by using Pohang city located in the East part of Korea as a test-bed example.

## 1. Introduction

Korea has been considered an earthquake-safe zone, but after the Gyeongju earthquake (M5.8, 2016) and the Pohang earthquake (M5.4, 2017), the seismic performance of the aging road infrastructures which are built based on old specifications or no earthquake-resistant design was doubted. This kind of anxiety was further amplified by the occurrence of 115 small and medium-sized earthquakes as shown in 2018 data of Korea Meteorological Administration. Starting from the earthquake disaster areas in Korea, an advanced method for the more reliable and quicker evaluation of the seismic performance of aging road facilities was requested, and it became a trigger to develop a seismic performance management system that can support the resilience management of the road network.

Decision support methods for seismic performance management of existing facilities are largely divided into deterministic and probabilistic methods. The deterministic method evaluates existing facilities' seismic performance using a determined specific earthquake, whereas the probabilistic method evaluates seismic performance taking into account various earthquake scenarios in order to overcome errors that may occur by standardizing the number of uncertain earthquake occurrences to a determined specific earthquake. The decision support technologies currently in use can be broadly classified into three categories: Indexes Method (NYSDOT, 2004), Expected Damage Method (FHWA, 2006), and the Seismic Risk Assessment Method (HAZUS-MH 2.1). The index evaluation method is a deterministic method that determines the priority by considering the amount of direct damage quantitatively and the degree of indirect damage calculated

**CORRESPONDENCE** Dongjoo Kim ✉ [djk776.kim@kalis.or.kr](mailto:djk776.kim@kalis.or.kr) ☒ Korea Authority of Land & Infrastructure Safety, Jinju 52856, Korea

© 2024 Korean Society of Civil Engineers

using the qualitative value of the seismic performance of individual facilities. The seismic risk assessment method, which is a probabilistic method, prepares various earthquake and traffic scenarios and quantitatively calculates the magnitude of direct and indirect damage through seismic performance analysis from the road network perspective for these scenarios. For example, Kang et al. (2008) proposed the matrix-based system reliability method and applied to bridge transportation network to evaluate the disconnection between each city and hospital under seismic conditions. Chen et al. (2023) conducted seismic risk assessment of bridge transportation network by employing betweenness centrality-based performance measure. In addition, Chen et al. (2022) presented a machine learning-based seismic reliability assessment methodology to accelerate system reliability computation time and Banerjee et al. (2019) introduced a comprehensive review on the multi-hazard resilience estimation of bridge transportation network. From the perspective of traffic flow analysis, Yoon et al. (2020) adopted Total System Travel Time (TSTT) as a network performance indicator and evaluated the seismic performance of a bridge transport network using an artificial neural network-based surrogate model. In addition, Yoon et al. (2021) proposed an optimal recovery strategy for bridge transportation networks by employing direct and indirect damage-based recovery priority indicators for seismic performance analysis. The decision-maker can choose a viable road network and determine the management budget based on these quantitative values.

The method mainly used in practice in Korea is Index Method (KALIS, 2011). This method suggests that the seismic performance of individual facilities can be evaluated sequentially, followed by preliminary and detailed evaluations. The decision-making necessary for seismic performance management is related to a preliminary evaluation, which calculates the seismic performance of individual facilities based on a qualitative index value. The Index Method supports only decision-making which is the priority of facilities needed for retrofitting or detailed evaluation. However, one fatal flaw is that seismic performance management is mainly conducted for individual facilities without considering the road network. This may result in the fact that the road network cannot be used immediately after the earthquake, despite actual seismic performance management. Therefore, the seismic performance of existing road facilities (bridges, tunnels, slopes, and retaining walls) should be efficiently managed with consideration of system-level performance in the post-earthquake stage, e.g., connectivity and traffic delay time (Lee and Song, 2023). In addition to prioritizing decision-making, there is a need for a method that can provide backup materials to support various and rational decision-making, such as budget setting and selection of earthquake safety roads. The proposed Seismic Risk Assessment method can provide the backup materials needed for various decision-making processes.

The purpose of this study is to verify the development technology by developing decision-making support technology for seismic management of old road facilities suitable for domestic conditions and applying it to Pohang city located in the East part of Korea as Test-Bed. In the companion paper (“Part 1), the seismic fragility

evaluation technology considering aging is studied for bridges, tunnels, retaining walls, and slopes. In this paper, the repair and reinforcement decision support system is studied. This system considers the degradation model of the structures and the recovery policy on the road network. In Section 2, the seismic risk assessment method is introduced for calculating direct & indirect damage of road networks, assessment of socio-economic resilience to disaster in South Korea, and method of decision-making. In Section 3, software for the decision-making system is presented. In Section 4, the application of developed technology and system is introduced.

## 2. Applied Ground Motions

Two pairs of ground motions recorded at the rock outcrops during the recent major earthquakes that occurred in Korea, i.e., the 2016 Gyeongju earthquake (M5.5) and 2017 Pohang earthquake (M5.4), were collected. To supplement, other five pairs of ground motions recorded in the USA, Greece, Japan, and Italy were also collected. Note that all of these ground motions were recorded at stations with epicentral distances shorter than 40 km. The information on the earthquakes associated with these ground motions is referred to in Seo et al. (2022). These selected ground motions are comparable to the design spectra of South Korea with return periods of 500 and 2,400 years. Note that the peak ground acceleration (PGA) of these motions varies from 0.11 to 0.43 g. No high-intensity earthquakes outside of this range have not been reported in Korea since the 20th century. However, to broaden the scope of this study to high-intensity earthquakes, it may be necessary to assess the additional seismic performance of damaged networks for aftershocks, while calculating the increased failure probabilities. The Seismic Risk Assessment calculates the direct damage (physical damage) of the road network for various earthquake scenarios through “seismic risk analysis”, and calculates the indirect damage (transport delay amount) for each restoration stage of the damaged road network through “traffic recovery analysis”. The quantified amount of direct and indirect damage can support various decisions.

### 2.1 Seismic Risk Analysis

Probabilistic seismic hazard analysis (PSHA) was first proposed by (Cornell, 1968), and many studies have been conducted in this regard. PSHA is evaluated as the probability of the occurrence of ground vibrations that can occur in the relevant area within a specific period. PSHA is evaluated through the following four steps: identification of seismic sources, quantification of seismic recurrence rate, attenuation models, and development of hazard curve, as indicated sequentially in Figs. 1(a) through 1(d).

#### 2.1.1 Identification of Seismic Sources

The first step of PSHA is to identify seismic sources from which earthquakes are expected to occur. Seismic sources are established based on seismic records and geographic evidence of the target area and its surroundings, which are classified into two types: 1)

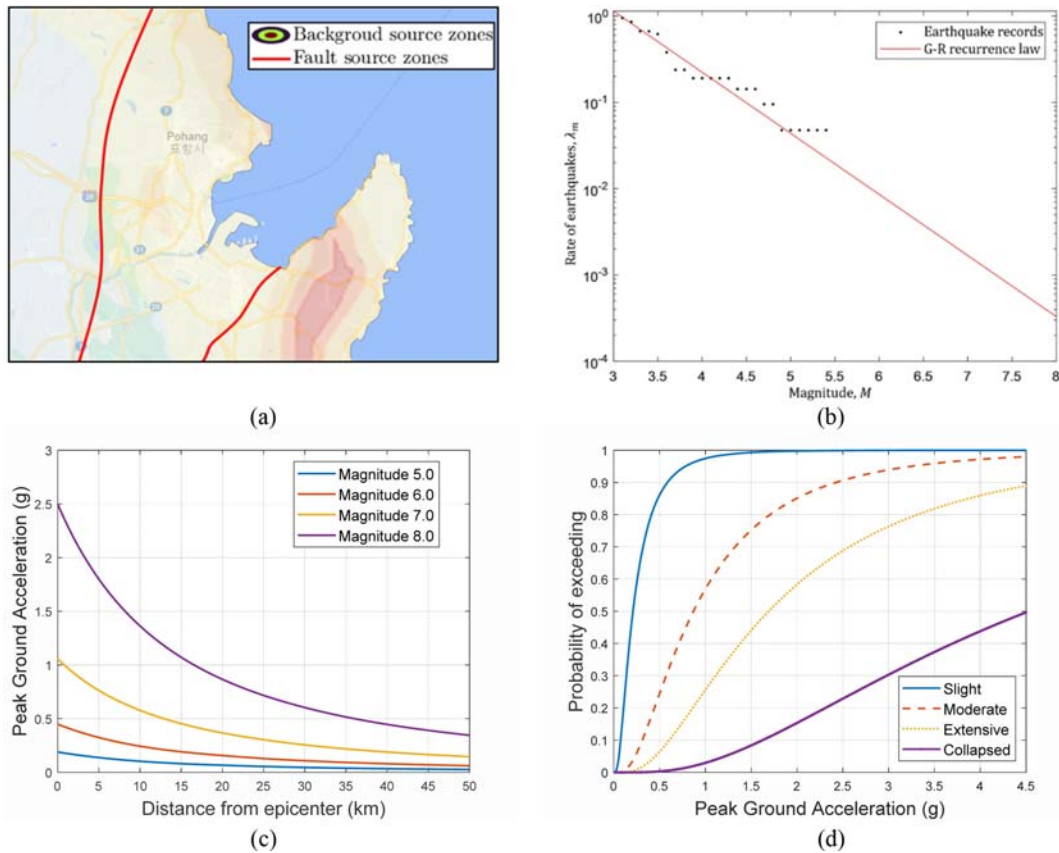


Fig. 1. Four Steps of Probabilistic Seismic Hazard Analysis (Kramer, 1996; Baker, 2008)

line or fault source zones (FSZs), and 2) area or background source zones (BSZs) (Sianko et al., 2020).

BSZs are introduced to quantify the seismic risk of areas that may experience significant earthquakes in the future for areas that do not have significant historical seismicity and do not know about near active faults. The region of interest is divided into appropriate BSZs and the potential seismic source locations within each zone are assumed to be completely random. In each established zone, the distribution of seismic magnitude is expressed by constant parameters of the Gutenberg-Richter (G-R) recurrence law (Gutenberg and Richter, 1944), which is described in detail in Step 2. Seismic catalog analysis for regions with fault segments differs from BSZ analysis in terms of the earthquake magnitude and annual frequency of occurrence. For FSZ analysis, the location of active faults in the region must be known in advance. Subsequently, starting with a newly observed seismic source, a line of potential seismic sources is established along the fault direction. In contrast to BSZ, it applies the seismic damping equation to the fault line generated using fault information rather than a single point in order to determine the seismic strength of a particular region close to the fault.

In seismically active areas with sufficiently accumulated earthquake records, the fault shape and rate of earthquake occurrence for each fault are well known, and the FSZ method can be easily used along faults. However, in other regions, it is usually difficult to estimate specific earthquake sources; therefore, the earthquake

source is set using the BSZ method. Fig. 1(a) shows an example of two active faults and the quantified seismic risk in Pohang for FSZ and BSZ methods, respectively.

### 2.1.2 Quantification of Seismic Recurrence Rate

After establishing seismic sources, the relationship between the expected earthquake magnitude and the occurrence rate for each source should be identified. The G-R recurrence law is one of the most used equations to estimate the frequency of earthquakes of a given magnitude, and is given as:

$$\log \lambda_m = a - bM, \quad (1)$$

where  $\lambda_m$  is the rate of earthquakes with magnitudes greater than  $M$ ; and the parameters  $a$  and  $b$  are constants determined from historical seismic data. Based on Eq. (1) and the earthquake records of the target area of this study (e.g., Pohang, Republic of Korea), the rate of earthquakes according to the magnitude is calculated in Fig. 1(b) (Tak et al., 2019).

### 2.1.3 Selection of Attenuation Models (GMPEs)

However, there is a limit to assessing seismic hazards accurately using only the seismic sources and magnitudes. To overcome this lack of information, ground-motion intensity measures such as peak ground acceleration (PGA), peak ground velocity (PGV), and spectral acceleration (SA) are utilized depending on the type of structure. A ground motion prediction equation (GMPE) is

generally evaluated in the following form (Abrahamson and Youngs, 1992; Joyner and Boore, 1993; Goda and Hong, 2008; Lim and Song, 2012; Lee and Song, 2021)

$$\ln D_i = f(M, R_i, \lambda_i) + X_i = f(M, R_i, \lambda_i) + \eta + \varepsilon_i, \quad (2)$$

where  $D_i$  is the seismic demand, also called a ground-motion intensity measure, at the  $i^{\text{th}}$  site;  $f$  is an attenuation relation given in terms of the earthquake magnitude  $M$ , the distance  $R_i$  between the earthquake source and the  $i^{\text{th}}$  site, and other parameters  $\lambda_i$ ; and  $X_i$  is a residual at the  $i^{\text{th}}$  site, with zero mean and standard deviation  $\sigma_{IM_i}$ . The residual  $X_i$  can be decomposed into the inter-event and intra-event residuals at the  $i^{\text{th}}$  site,  $\eta$  and  $\varepsilon_i$ .  $\eta$  and  $\varepsilon_i$  account for the uncertainty of individual earthquakes and spatial distribution, respectively.

That is, for a single earthquake scenario,  $\eta$  has the same value for all structures in the given bridge network, while  $\varepsilon_i$  has a different value for each structure. In general, PGA is used as the ground-motion intensity measure for road facilities covered in this study (Lim and Song, 2012). The attenuation model for the PGA demand is given by (Cornell et al., 1979):

$$f(M, R_i, \lambda_i) = \lambda_{D_i} = -0.152 + 0.859M - 1.803 \ln(R_i + 25), \quad (3)$$

where  $\lambda_{D_i}$  is the predicted natural logarithms of PGA demand at the  $i^{\text{th}}$  site. Fig. 1(c) visualizes the changes in  $\lambda_{D_i}$  as  $R_i$  varies for different earthquake magnitudes. The standard deviations of  $\eta$  and  $\varepsilon_i$  are assumed to be 0.254 and 0.512, respectively.

#### 2.1.4 Development of Hazard Curves

By combining the seismic capacity of components in the road network with the information about the seismic demands (e.g., location of seismic sources, recurrence rate by earthquake magnitude, PGAs predicted from an attenuation model, discussed in previous sections), one can assess seismic performance or hazards such as the probability of exceedance. When the seismic capacity of the  $i^{\text{th}}$  structure,  $C_i$ , follows a lognormal distribution (i.e.,  $\ln C_i$  follows a Gaussian distribution), the failure probability of the structure is described as follows:

$$P_i = P(C_i \leq D_i) = \Phi\left(\frac{\lambda_{D_i} - \lambda_{C_i}}{\sqrt{\zeta_{C_i}^2 + \zeta_{D_i}^2}}\right), \quad (4)$$

where  $P_i$  is the failure event of the  $i^{\text{th}}$  structure;  $\Phi(\cdot)$  denotes the cumulative distribution function of the standard Gaussian distribution;  $\lambda_{C_i}$  is the mean of  $\ln C_i$ ;  $\zeta_{C_i}$  and  $\zeta_{D_i}$  are the standard deviations of  $\ln C_i$  and  $\ln D_i$ , respectively. As shown in Fig. 1(d), multi-state structures have fragility curves for each of the states for the given ground-motion intensity measure.

#### 2.1.5 Direct Damage

As shown in Eq. (5), the direct damage can be calculated by the probability of excess for each damage class of individual road facilities shown in Eq. (4), and the damage cost ratio for each damage class. In this study, the damage cost of the relevant facility is calculated as the ratio of construction costs.

$$DC_{k,m} = \sum_{m=1}^N \left[ RE_i \times \sum_{m=1}^N \sum_{ds=1}^{DS} (RCR_m^i \times P_{ds}^{i,k,m}) \right], \quad (5)$$

where  $DC_{k,m}$  is the cost of direct damage to the road network for the recurrence period ( $k$ ) and the epicenter scenario ( $m$ ),  $RE_i$  is the replacement cost of the facility,  $DS$  is the damage level structure,  $RCR$  is the repair cost converted as a percentage of the facility construction cost, and  $P_{ds}$  denotes the probability of each damage class.

## 2.2 Resilience Assessment of Road Network

The number of cases of road network damage is determined by a combination of five damage levels (no damage, minor, moderate, severe, and collapsed) of individual facilities included in the road network, and the amount of traffic delay is calculated through resilience assessment of the road network for each combination. Various algorithms have been proposed for the resilience assessment of road networks (Kang et al., 2008; Banerjee et al., 2019; Chen et al., 2022; Chen et al., 2023), and Monte Carlo Simulation (MCS) is one of the straightforward and most widely used methods. The MCS calculates the amount of traffic delay by sampling the damage level of the road network, and increases the number of samples to converge the amount of traffic delay for a specific earthquake.

However, the number of cases of damage level for the  $N$  facilities with 5 damage levels is  $5N$ , and analyzing the damage level of the road network with a large number of road facilities through Monte Carlo simulation takes a long time, so it can be said that it is inappropriate for the seismic performance evaluation of a complex road network. In order to overcome this problem, a method for evaluating the level performance of a road network using an artificial neural network-based surrogate model was developed.

### 2.2.1 System-Level Performance Evaluation of Transportation Network Employing ANN-Based Surrogate Model

For optimal decision-making immediately after an earthquake, rapid evaluation of the degraded performance of a bridge transportation network is important. For the task, an ANN-based surrogate model is introduced. An ANN technique typically recognizes patterns in input data through supervised learning and expresses complex relationships between input and output data with mathematical functions. Since the handling of an ANN algorithm is relatively simple, numerous researchers have been using ANN algorithms in various research fields such as structural health monitoring (Rizzo and Lanza di Scalea, 2006), vibration control (Akin and Sahin, 2017), damage detection (Nguyen et al., 2019), and structural response analysis (Onat and Gul, 2018).

In a previous study, an ANN-based surrogate model was constructed for the accelerated seismic risk assessment of a bridge transportation network, and the total system travel time (TSTT) was adopted as a performance index (Yoon et al., 2020). Although TSTT may have high accuracy in performance assessment

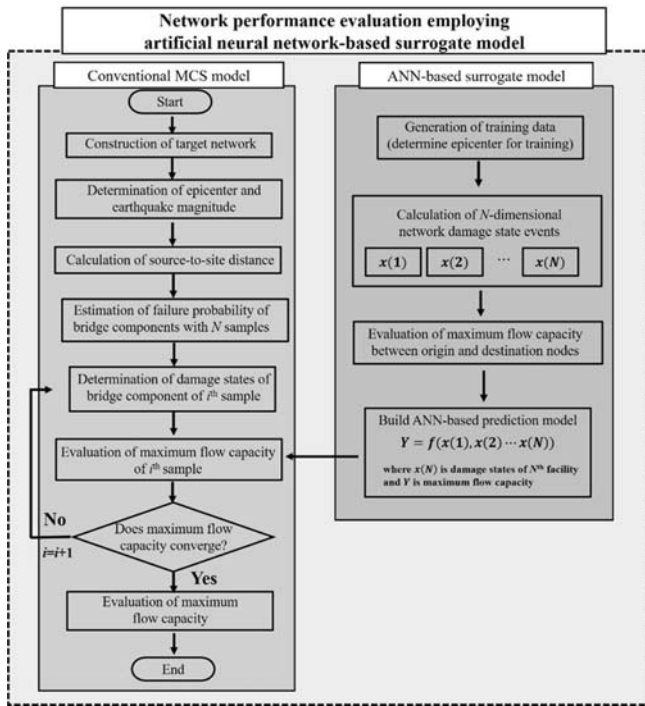


Fig. 2. Flowchart of Network Performance Evaluation

results, the computational cost can be high. For this reason, in this study, the maximum flow capacity (i.e., the maximum number of passing vehicles per unit time) is introduced to measure the system-level performance of a transportation network, and MATLAB Boost Graph Library (Boost, 2008; Gleich, 2008) is used to calculate the maximum flow capacity.

Figure 2 shows the overall flowchart of the method introduced for this study. First of all, for network analysis, a network map should be constructed using topological data (including node locations, links, and node connectivity information in terms of an adjacent matrix) so that it can be introduced into a geographic information system (GIS).

After a network map is constructed, an ANN-based surrogate model is trained by determining the earthquake epicenters and magnitudes based on historical earthquakes. Once epicenter locations and magnitudes of earthquakes are determined, the ground motion at a specific location from an epicenter can be predicted using the ground motion prediction equation (GMPE) and spatial correlation, and the damage probability of a bridge structure can then be calculated according to the intensity measure. For ground motion prediction, the GMPE proposed by Cornell et al. (1979) was utilized in Eq. (3). In addition, inter-event and intra-event terms are introduced to represent the uncertainty of the ground motion. Inter-event represents the uncertainty of predicted ground motion intensity owing to the characteristics of seismic waves themselves, and intra-event represents the uncertainty of predicted ground motion intensity depending on the geotechnical environment and seismic propagation path. The total uncertainty of the ground motion,  $\rho_{total}$ , can be explained by the following equation (Sokolov et al., 2010):

$$\rho_{total} = \frac{\sigma_{\eta}^2}{\sigma_{\eta}^2 + \sigma_{\epsilon}^2} + \frac{\sigma_{\epsilon}^2}{\sigma_{\eta}^2 + \sigma_{\epsilon}^2} \rho(\Delta_{ij}), \tag{6}$$

where  $\sigma_{\eta}$  and  $\sigma_{\epsilon}$  denote the inter- and intra-event standard deviations with zero means, and  $\rho(\Delta_{ij})$  denotes the spatial correlation equation. In this study, the following equation proposed by Goda and Hong (2008) is utilized:

$$\rho(\Delta_{ij}) = e^{(-0.509 \cdot \sqrt{\Delta})}, \tag{7}$$

where  $\Delta$  denotes the distance between two location sites  $i$  and  $j$ .

The next step is to obtain the damage probability of a bridge structure according to the ground motion intensity. Federal Emergency Management Agency (FEMA) suggests that SA is the best predictor of bridge damage probability among various intensity measures. In addition, based on historical data, the seismic fragility curves of various bridge types are also suggested for five damage states using lognormal distributions by providing the associated medians and log standard deviations (Yoon et al., 2020) which are introduced into this study.

To represent the performance degradation of damaged bridges in a transportation network, the damaged bridges are often modeled with their reduced traffic capacities according to the damage states. In this study, the traffic capacities according to the five damage states proposed by Mackie and Stojadinovic, 2006 are adopted. Table 1 shows the reduced traffic capacities, which are quarter-based from 0 – 100% of the original capacity of an intact bridge.

Once the damage states of bridge structures are determined and the traffic capacities are modified accordingly, the performance of a bridge transportation network can be evaluated in terms of the maximum flow capacity, using the MATLAB Boost Graph Library (Boost, 2008; Gleich, 2008). Based on the evaluation results, an ANN-based surrogate model is constructed to represent the relationship between the damage states of bridge structures and the system-level network performance. The constructed surrogate model can accelerate the calculation of the maximum flow capacity for each sample earthquake scenario which represents the occurrence of an earthquake at an epicenter with a random magnitude. When the average maximum flow capacity calculated in this way converges, the final network performance is calculated and the analysis is terminated.

Table 1. Modified Traffic Capacities according to Damage States of Bridges (Mackie and Stojadinovic, 2006)

Damage state	Modified traffic capacity
No damage	100%
Slight damage	75%
Moderate damage	50%
Extensive damage	25%
Complete damage	0%

### 2.2.2 Seismic Resilience Assessment of Bridge Transportation Network

Section 2.2.1 describes a method using an ANN-based surrogated model for accelerating the performance evaluation of a transportation network considering damaged bridges. This section addresses the recovery of a bridge transportation network following the restoration of damaged bridge structures after an earthquake. Finally, a methodology providing the seismic resilience curve of a bridge transportation network over time is proposed

Figure 3 shows the flowchart of the seismic resilience assessment for bridge transportation networks employing an ANN-based surrogate model. The main difference from the method described in the previous section is that an additional step is introduced to calculate the time required for the recovery of each damaged bridge, and through the recovery model, the proposed method calculates the updated maximum flow capacity based on the updated damage states. FEMA presented the required restoration period according to the bridge damage state (FEMA, 2003), which is introduced in this study and shown in Table 2.

As described in Section 2.2.1, when a target transportation network is constructed, and the epicenter and earthquake magnitude

**Table 2.** Damage State and Required Restoration Period of Bridge Structure (FEMA, 2003)

Damage state	Required restoration period [Days]
No damage	0
Slight damage	0.6
Moderate damage	2.5
Extensive damage	75
Complete damage	230

are determined, for each of  $N$  random samples, the damage states of bridges and the required restoration periods corresponding to the damage states can be determined. The maximum flow capacity can be calculated using the constructed ANN-based surrogate model whenever the traffic capacity changes according to the restoration of damaged bridges. The seismic resilience curve for a target bridge transportation network is obtained through this iterative process.

### 2.2.3 Indirect Damage

To calculate the indirect damage, it is necessary to calculate the additional traffic volume due to road detours. The additional

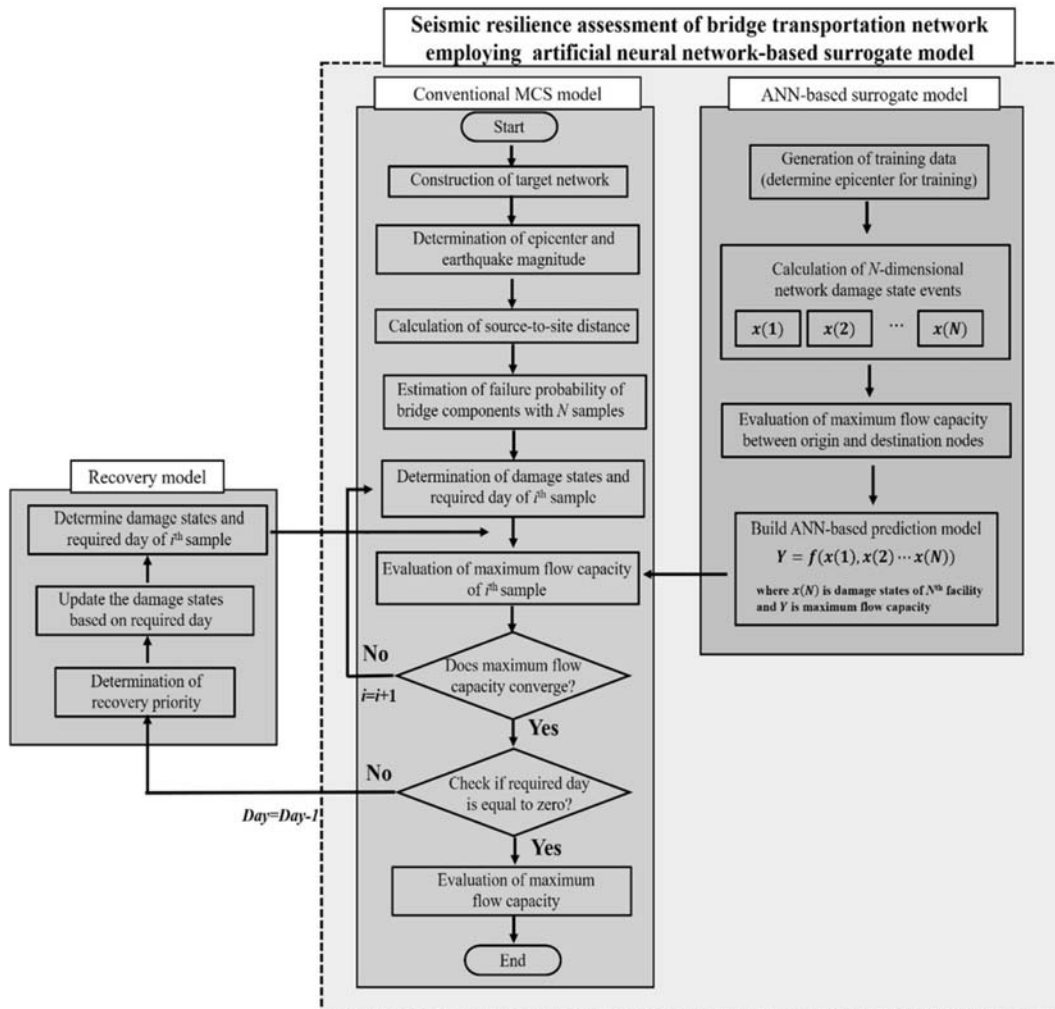


**Fig. 3.** Flowchart of Seismic Resilience Assessment of Bridge Transportation Network Employing ANN-Based Surrogate Model

**Table 3.** Objective and Factor of Socio-Economic Resilience by Each Stage

Stage	Objective	Factor	
Damage Stage	Minimize damage caused by disasters through reducing exposure and impact of individual, industry, and facility to disaster	Social resilience	• Demographic characteristic
		Economic resilience	• Economic stability • Industrial stability
		Physical resilience	• Physical robustness
Recovery Stage	Rapid and efficient recovery activities to prevent prolonged direct or indirect damage from disaster	Social resilience	• Demographic characteristic • Community capacity
		Economic resilience	• Economic stability • Industrial stability
		Physical resilience	• Physical robustness • Response infrastructural capacity
		Institutional resilience	• Administrative capacity • Capacity for disaster management

traffic volume is calculated by comparing the total traffic before and after the earthquake and the time it took to pass through a set of origins and destinations. In contrast to the direct damage cost calculation, indirect damage calculation should consider the road network restoration stage as shown in Sections 2.2.1 and 2.2.2. Until the road network is normalized, the additional traffic volume can be calculated from the first stage with the largest amount of additional traffic to the last stage with no additional traffic volume. The total cost of damage due to traffic delays in the road network can be calculated using Eq. (8) below.

$$TC_{(p)} = VOT \times \sum_{j=1}^{Link} (TC_{j,p} - TC_{j,0}), \quad (8)$$

where  $TC_{(p)}$  is the cost of damage caused by the total traffic delay of the road network,  $p$  is the state of recovery,  $j$  is the route number,  $VOT$  is the cost of delay per hour,  $TC_{j,p}$  is the traffic volume for route  $j$  and recovery state  $p$ ,  $TC_{j,0}$  is the traffic volume for route  $j$  under normal conditions.

## 2.3 Assessment of Socio-Economic Resilience to Disaster in South Korea

### 2.3.1 Socio-Economic Resilience Index to Disaster

In our study, we define socio-economic resilience as the regional ability to minimize damage and efficiently recover from a disaster. Socioeconomic resilience consists of four dimensions: social, economic, institutional, and physical resilience. We conceptualize each dimension: social resilience (SR), which refers to the level of exposure of individuals and local communities to disaster and the ability to participate in the recovery process; economic resilience (ER), which refers to the financial condition of the region for supporting recovery and industrial stability, professionalism, and innovativeness against disaster risks; physical resilience (PR), which refers to the disaster response facilities' physical robustness; and institutional resilience (IR), which refers to the regional administrative capacity or disaster response agency's ability to support disaster response activities.

We also divided resilience into two phases: damage occurrence and recovery from the disaster (Table 3). In the damage stage, resilience can minimize the occurrence of damage and prevent the spread of disaster damage. During the recovery stage, resilience can affect rapid and efficient recovery from disasters to prevent prolonged disaster damage. Thus, socioeconomic resilience can be secured by minimizing damage from disasters and efficiently recovering from disasters at the regional level.

According to the conceptualization of socio-economic resilience, we analyzed the main factors for securing resilience at each stage. In the damage stage, resilience can be improved by reducing the exposure and impact of targets such as residents, industries, and facilities that may be affected by disaster damage, thereby minimizing the damage from disasters. As a result, we identified the following factors as the most important: demographic characteristics that can affect residents' exposure to and impact from disaster (social resilience), economic and industrial stability (economic resilience), and physical robustness of local facilities against disaster (physical resilience). In the recovery stage, resilience can be improved by quick and efficient recovery from disaster damage.

Therefore, we also defined factors as main factors such as demographic characteristics and community capacity that support recovery activities (social resilience); economic abundance that supports recovery activities and industrial stability or diversity that revitalize the industry and create innovations from disasters (economic resilience); physical robustness of local facilities against disaster (physical resilience), and administrative capacity to manage the overall recovery process and response activities (institutional resilience).

We developed evaluation indicators for socioeconomic resilience assessment according to the main factors at each stage. For the social resilience assessment, we developed three indicators of demographic characteristics and four indicators of community capacity. For economic resilience, we developed 4 economic stability indicators and 5 industrial stability indicators. For physical resilience, we developed three indicators of physical robustness and three indicators of emergency response infrastructure capacity.

**Table 4.** Evaluation Indicators of Socio-Economic Resilience

Dimension	Sub-category	Keyword	Indicator	Unit		
Social Resilience	Demographic characteristic	Education	Ratio of residents highly educated	%		
		Health	Ratio of health risk group	%		
		Vulnerability to disaster	Ratio of the vulnerable to disaster	%		
	Community capacity	Participation (and Cohesiveness) in volunteering activities	Participation (and Cohesiveness) in volunteering activities	Ratio of participation in volunteering	%	
			Supplement of volunteering activities	Number of enrolled volunteers per 1,000 people	-	
			Supplement of volunteering activities	Ratio of volunteering activity support budget	%	
Respondable population		Respondable population	Ratio of young adults and middle-aged people (15 – 64 years old)	%		
	Economic stability	Income	Average monthly income per capita	won		
		Participation in economic activities	Number of employees per business	-		
Financial status of local government		Ratio of Financial independence	%			
Industrial stability	Diversity of industrial structure	Total budget	Total budget	won		
		Diversity of industrial structure	DII (Diversity index of income) in regional industries	-		
		Size of industrial structure	Total GRDP per capita	-		
	Usable labor force	Usable labor force	Ratio of working age population	%		
		Innovative industry	Ratio of higher value-added industries	%		
		Innovative industry	Ratio of budget for supporting R&D	%		
Physical Resilience	Physical robustness	Building safety code	Facility safety score	-		
		Building ages	Ratio of old buildings	%		
		Vacant houses (abandoned houses)	Ratio of vacant houses	%		
	Response Infrastructural capacity	Supplement of shelter	Supplement of shelter	Number of shelters per 1,000 people	-	
			Accessibility in region (In and Out)	Ratio of road pavement	%	
			Accessibility in region (In and Out)	Extension length of road per regional area	km	
Institutional Resilience	Administrative capacity	Manpower for government service	Manpower for government service	Number of public officials per 1,000 people	-	
			Social assistance	Social assistance	Number of workers in social welfare facilities per 1,000 people in the vulnerable class	-
				Social assistance	Ratio of budget for social welfare	%
	Capacity for disaster management	Budget for disaster management	Budget for disaster management	Ratio of budget related to disaster management	%	
			Manpower for disaster management	Manpower for disaster management	Number of public officials in disaster management department per 1,000 people	-
				Medical capacity	Number of hospital beds per 1,000 people	-
		Emergency response capacity	Emergency response capacity	Emergency response capacity	Number of medical personnel per 1,000 people	-
				Emergency response capacity	Number of police station per 1,000 people	-
				Emergency response capacity	Number of fire station per 1,000 people	-

For institutional resilience, we developed three indicators of institutional capacity and six indicators of emergency response organizational capacity (Table 4).

### 2.3.2 Estimation of Weight of Socio-Economic Resilience Index

To estimate the weight of each evaluation indicator, we applied the entropy weight methodology. The entropy weight methodology is a method of calculating weights using the attribute of an index based on information theory. In this method, the higher the cohesion of the indicator value, the higher the weights that are calculated. The advantage of the entropy weight methodology is that subjectivity, which is a limitation of the Delphi method

and AHP method based on expert surveys, is excluded. In addition, it can help with an objective analysis that reflects only the characteristics of quantitative data (Lee et al., 2015). The entropy weight is calculated as follows: To estimate the entropy weight, we first estimated the value of the standardization of indicators  $p_{ij}$  (Eqs. (9), (10)) and calculated the entropy weight  $W_j$  like below (Eq. (11), (12)).

$$D = \begin{matrix} x_{11} & \cdots & x_{1n} \\ \vdots & & \vdots \\ x_{m1} & \cdots & x_{mn} \end{matrix} \quad (9)$$

$m$ : Num of Regions

$n$ : Num of variables

$$P_{ij} = \frac{x_{ij}}{\sum_{i=1}^m x_{ij}} \quad (i = 1, 2, \dots, m; j = 1, 2, \dots, n) \quad (10)$$

$$E_j = -k \sum_{i=1}^m p_{ij} \log p_{ij} \left( k = \frac{1}{\log m}; j = 1, 2, \dots, n \right) \quad (11)$$

$$d_j = 1 - E_j$$

$$W_j = \frac{d_j}{\sum_{j=1}^n d_j} \quad (j = 1, 2, \dots, n) \quad (12)$$

$d_j$ : Degree of diversity

$w_j$ : Entropy weight

In our study, we also used the analytical hierarchy process (AHP) for estimating the weight values based on the knowledge and experience of experts. AHP is based on developing a hierarchal presentation of the decision-making problem and then analyzing this hierarchy through a series of pairwise comparison judgments to express the relative strength or intensity of hierarchy elements (Saaty, 1987; Aomar, 2010).

By combining both the AHP weight and entropy weight, we estimated the integrated AHP-Entropy weight by each indicator. Entropy weight methodology can derive effective and depict weight values, but it relies heavily on the objective data that ignores the knowledge and experience of the experts (Nyimbili and Erden, 2020). Considering the entropy only, irrespective of the expert's perspective would be insufficient and may not always accurately reflect the importance of the indicator in practice (Zardari et al., 2015). Therefore, we combined the subjectivity of the AHP and the objectivity of the entropy weight methodology to estimate weight by each indicator (Eq. (13)). Integrated AHP-Entropy weight is calculated from the AHP and Entropy weighting procedure using the general form of the Shannon entropy weight  $W_k^*$  given by the following equation: where  $S_j$  is the subjective weight calculated from the AHP, and  $W_j$  is the objective weight derived from the Entropy method (Nyimbili and Erden, 2020) (Eq. (13)).

$$W_j^* = \frac{S_j W_j}{\sum_{j=1}^n S_j W_j} \quad (13)$$

### 2.3.3 Quantification of Socio-Economic Resilience

We estimated the socio-economic resilience of each Si-Gun-Gu region in South Korea using socio-economic resilience indicators by each dimension such as social resilience (SR), economic resilience (ER), physical resilience (PR), and institutional resilience (IR) (Eq. (15)). To estimate socio-economic resilience, all indicators ( $X_i$ ) were normalized using min-max normalization (Eq. (14)), and the normalized values ( $M_i$ ) were multiplied by integrated AHP-Entropy weights. To quantify socio-economic resilience, we summed the value of each dimension of resilience (Eq. (16)).

$$M_i = \frac{X_i - X_{min}}{X_{max} - X_{min}} \quad (14)$$

$$\text{Social Resilience}(SR) = \frac{\sum_n (W_j^* \times I_{sr-j})}{\text{number of indicators}}$$

$$\text{Economic resilience}(ER) = \frac{\sum_n (W_j^* \times I_{er-j})}{\text{number of indicators}} \quad (15)$$

$$\text{Physical resilience}(PR) = \frac{\sum_n (W_j^* \times I_{pr-j})}{\text{number of indicators}}$$

$$\text{Institutional resilience}(IR) = \frac{\sum_n (W_j^* \times I_{ir-j})}{\text{number of indicators}}$$

$$\text{Socioeconomic resilience} = SR + ER + PR + IR \quad (16)$$

## 2.4 Decision-Making

### 2.4.1 The Method of Decision-Making

The magnitude and frequency of earthquakes are increasing owing to the recent acceleration of climate change. Therefore, multi-faceted efforts are needed to prevent the loss of infrastructure in road networks by probabilistically analyzing the characteristics of potential earthquakes based on the PSHA. In particular, there is a need for a method to precisely identify and minimize losses due to earthquakes. The following studies emphasize that it is possible to prepare for unexpected incidental losses after an earthquake through accurate loss assessment by considering indirect damage at the urban system level as well as repair and reinforcement according to the link status in the infrastructure road network.

Sohn et al. (2003) introduced a loss analysis model suitable for each part by dividing the direct and indirect damage into an economic part and a non-economic part. In particular, for indirect cost calculation, the region was divided into several zones according to regional characteristics, and the cost model calculated using socioeconomic indicators in each zone was used. Du and Peeta (2014) proposed a stochastic optimization model that minimizes the recovery time after a disaster by injecting a limited budget before a general disaster. By taking into account the road network's connectivity, each link's function in the context of traffic flow, and the marginal survivability boosted by investment, it is currently possible to give decision-makers a process that reflects the full characteristics of the road network. In the optimization model, it is characteristic that investment decisions for non-dependent links are regarded as continuous variables. Sextos et al. (2017) proposed an index that quantifies the direct and indirect damage to the road network due to an earthquake and explained that social loss after an earthquake can be greatly reduced through the pre-reinforcement of appropriate links.

In this paper, we proposed that quantitative indices, such as the cost of reconstruction and delay time of transportation during the scheduled for repair of the road damaged by the earthquake, be considered, as shown in Fig. 4. The construction cost is derived from the fragility curve, which includes the aging effect of facilities, and the delay time of transportation is calculated using an ANN-based surrogate model that can handle complex road networks.

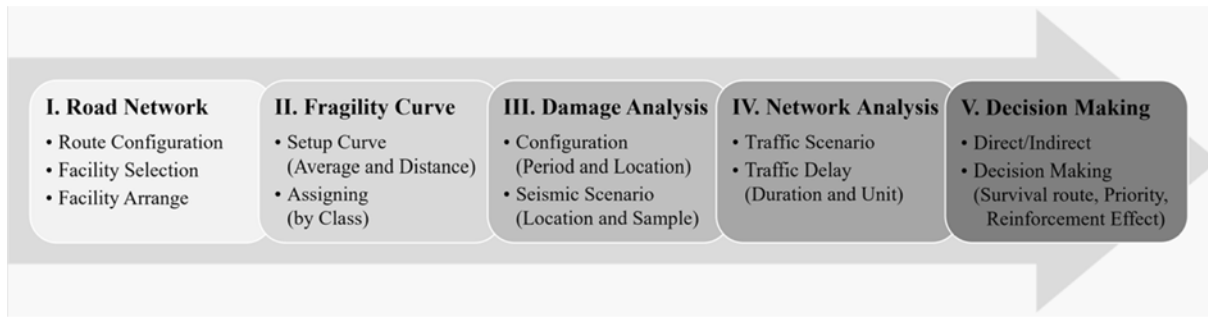


Fig. 4. Five(5) Steps of Decision-Making

### 2.4.2 The List of Decision-Making

In this study three decision-makings, priority for seismic reinforcement, necessary budgeting, and selection of disaster prevention roads, are proposed. First, seismic reinforcement should be carried out for all facilities that are not designed for seismic resistance. However, because of the limited budget, it is impossible to reinforce the seismic performance of all facilities at once. Therefore, it is necessary to prioritize the reinforcement of seismic performance management such that the set budget can be used effectively. Currently, the method primarily used in seismic performance management practice suggests the priority of seismic reinforcement for individual road facilities. However, the improvement of the seismic performance of individual facilities does not mean the improvement of the seismic performance of the road function of the road network. In this study, to improve the seismic performance of road functions, the priority of seismic reinforcement focused on the road network was proposed so that the seismic performance management of existing facilities from the perspective of the road network could be achieved. Second, it is important to preemptively set the budget necessary for seismic performance

management. The required budget can be estimated according to the method of prioritizing seismic performance management. As a decision-making process, a method to estimate the budget for seismic reinforcement of the route of interest is presented.

Finally, the selection of a disaster prevention road is proposed. Various standards are proposed in Korea for the selection of disaster prevention roads, but qualitative values are used as standards, considering the importance of roads and lane clearance without quantified standards. One of the advantages of the Seismic Risk Assessment Method is the evaluation of the rate of road functions on specific routes, based upon quantitative direct and indirect damage. With quantitative results, more objective and reasonable decision-making for disaster and road prevention can be performed. The decision-making items proposed in this section is executed using the developed software introduced in the next section.

### 3. Decision Support Software for Seismic Performance Management

It is necessary to overcome the limitations of the Index Method,

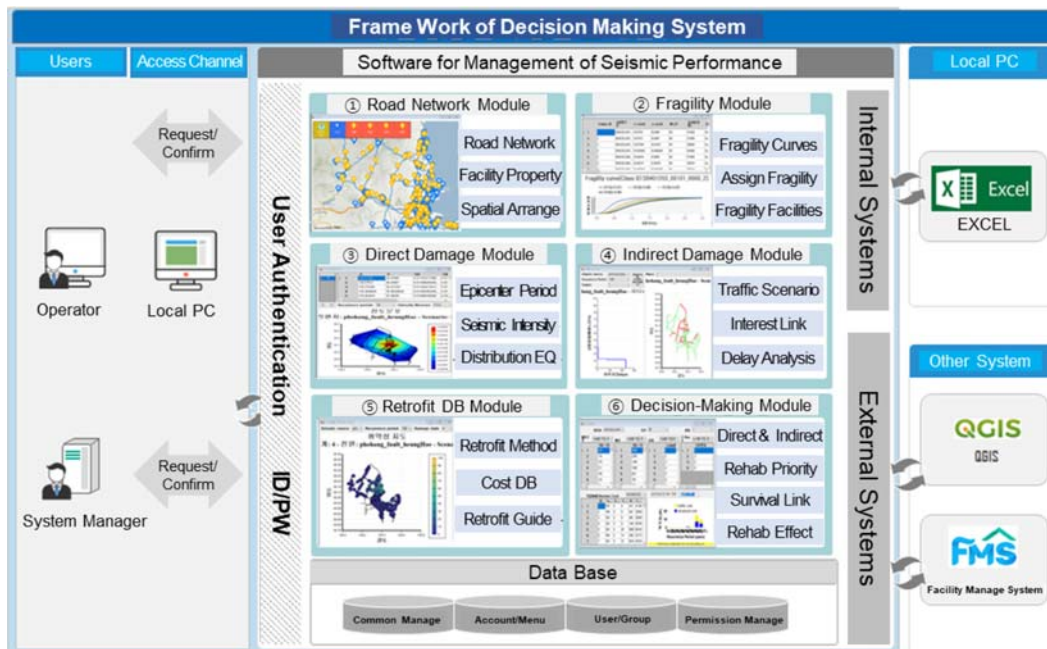


Fig. 5. Modules of the Decision-Making Platform

which is mainly used in seismic performance management practice, and to switch to the Seismic Risk Assessment Method that can provide various judgment data necessary for decision-making. However, the Seismic Risk Assessment Method requires many calculations to produce various judgment data and requires specialized knowledge of the use of the evaluation results. So, as shown in Fig. 5, spatial information-based software was created as a tool to assist decision-makers in easily understanding and utilizing the outcomes of the seismic risk assessment method.

Decision support software consists of six (6) modules: road network configuration, fragility, direct damage, indirect damage, retrofit DB, and decision-making. The road network module enables users to input/output spatial information of the road network and the properties of the facility in the seismic performance management area. The fragility module is designed to assign proper fragility curves to road facilities using the “Part I Fragility Curve”. The fragility module works in conjunction with the direct damage module to calculate the magnitude of damage to road facilities for each earthquake scenario based on the location of faults in the proximity of the road network and earthquake intensity by return year. The indirect damage module calculates the volume of traffic delay using Monte Carlo Simulation and an artificial neural network (ANN)-based Surrogate Model. The user may select Monte Carlo Simulation for a simple road network, and Surrogate Model for a complex road network. In the Retrofit DB module, the retrofit method and cost were provided so that the user can select the proper method with its typical costs. Finally, the decision-making module was developed to provide tables and graphics so that various decisions can be made intuitively based on the materials generated in the 1 – 5 modules. In the decision-making module, qualitative data such as Socio-Economic Resilience derived in Section 2.3 is also provided for reference.

### 4. Field Application of Test Bed

#### 4.1 Road Network of Test Bed and OD Link

To verify the seismic risk assessment method developed in this study, support technologies were applied to the road network in Pohang, which is located in the eastern part of Korea where the recent earthquake occurred. A road network consisting of 426 nodes (nodes) and 1285 routes was constructed. Routes with two or more lanes in Pohang were selected. The road facilities in Pohang consist of 351 bridges, 43 tunnels, 70 slopes, and 25 retaining walls. Among these facilities, 220 bridges, 16 tunnels, 16 slopes, and 10 retaining walls, were included in the developed road network, as shown in Fig. 6.

The road network should be maintained so that the functions of the OD (origin-destination) routes are working at all times. OD

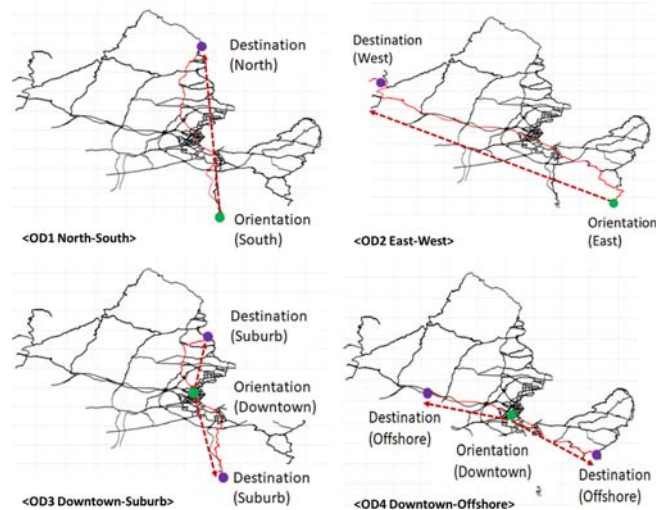


Fig. 7. Four(4) OD (Origin-Destination) Route

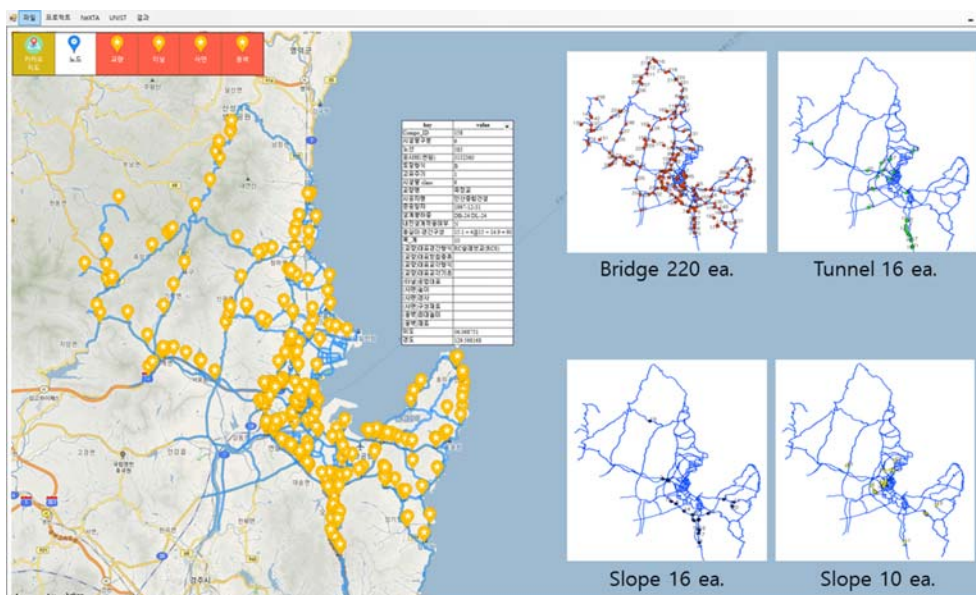


Fig. 6. Applicable Road Facilities in Pohang

**Table 5.** Actual Damage versus Simulated Damage

Return Year	Damage Type	Actual (mil KRW)	Simulated (mil KRW)
475	Direct	4,500	6,500
	Indirect	-	2,500

routes are the shortest routes from the starting point to the destination that drivers can use. Fig. 7 shows the 4 (four) OD routes. Since the purpose of decision-making is for minimizing the damage of earthquake, origination of OD routes was selected from the area where direct and indirect damage is highly expected and destination of OD routes from the the area of safety in outskirts of the city. OD1 is for transporting from fault dense area to non-fault area, OD2 for transporting from the downtown area to the suburbs or the offshore (OD3), and OD4 for transporting from the inland to the offshore. OD1 includes 33 facilities, OD2 includes 22 facilities, OD3 includes 10 facilities, and OD4 includes 11 facilities.

## 4.2 The Result of Test Bed

### 4.2.1 Actual Damage versus Simulated Damage

The reliability of the developed technology was verified by comparing the actual and simulated damages of individual facilities. Table 5 shows the actual damage and simulation damage of the road facilities in Pohang. Because actual damage was counted for direct damage only, a limited review comparing direct damage was conducted.

As a result of the comparison, the direct damage through the simulation was calculated to be somewhat larger than the actual damage. Since simulated damage includes additional damage of potential road facilities for a total of 262 facilities other than the 11 facilities shown in the ‘‘Pohang Earthquake Public Facility Damage Investigation’’, and the purpose of budget review which is preemptive measures to prevent loss of function. Considering the uncertainty of earthquakes, it is considered to be a sufficiently reasonable result that meets the purpose of establishing the system, ‘‘supporting decision-making for seismic performance management.’’

### 4.2.2 The Effect of Seismic Retrofit

The fragility functions are designed to consider the types of superstructure, substructure, bearing, seismic design, foundation, ground condition and deterioration. Therefore, retrofitting can be simulated by selecting fragility function which consider bearing replacement (from steel bearing to elastomeric bearing), pier reinforcement (section enlargement or Jacketing), and foundation reinforcement (adding mini pile). Using the developed software, cases of full retrofitting and non-retrofitting are simulated and compared to determine the effect of retrofitting. Table 6 shows the results of this comparison. It was found that the seismic retrofit is more effective for an earthquake with 475 return years, rather than 1000 return years.

**Table 6.** The Effects of Seismic Retrofit (mil. KRW)

Return Year	Damage Type	Before Retrofit	After Retrofit	Effect
475	Direct	6,500	3,300	3,200
	Indirect	2,900	1,800	1,100
1000	Direct	82,00	51,500	30,500
	Indirect	64,00	38,400	22,600

**Table 7.** The Direct and Indirect Damage of the OD Routes (mil. KRW)

Road Link	475 Return Year		
	Direct	Indirect	Sub total
OD1	450	540	990
OD2	620	270	890
OD3	170	1,090	1,260
OD4	610	530	1,140

### 4.2.3 Priority for the Retrofit of OD Routes

The magnitude of the total damage to the four previously selected OD routes was calculated, and the route with the most damage was prioritized for seismic retrofitting. Table 7 shows the direct and indirect damage of the OD routes.

The total damage of the OD routes is shown in Table 7, and the priority for seismic retrofitting of the routes was investigated in the order of OD3, OD4, OD1, and OD2.

### 4.2.4 Decision-Making on the Selection of Disaster Prevention Route

Various standards have been proposed for the selection of disaster prevention roads, but qualitative values are used as standards, considering the importance of roads and lane clearance. One of the advantages of the decision-making support software developed in this study is that the status of road function after an earthquake and the cost of retrofitting a specific route can be quantified, which provides a more objective and reasonable selection of disaster prevention roads. When selecting a disaster prevention road among the four OD routes, the criterion to be considered first is the minimum damage in the traffic function. Since the order of indirect damage is OD4, OD3, OD1, and OD2, the OD2 route can be prioritized for retrofitting among the candidates for disaster prevention roads. In this paper, only four OD routes were used for the simulation, but the number of OD routes can be increased for more reasonable and economic disaster prevention routes.

## 5. Conclusions

The seismic evaluation method that is mainly used in seismic performance management practice is the Index Method. With the Index Method, the seismic performance of individual facilities is calculated as a qualitative index value, and only priority decision-making for seismic performance management is supported according to the size of the index value. It is not possible to provide

materials such as direct and indirect damages, the required budget, and the effect of retrofit, which are needed for various decision-making processes. In addition, since the priority of retrofitting is determined based on individual facilities without considering the road network, roads may not perform normal traffic functions during earthquakes even after retrofitting. Therefore, it is necessary to use the Seismic Risk Assessment Method which can provide the various materials needed for decision-making.

In the probabilistic seismic hazard analysis, the probability of the ground excitations within a specific period is computed for the area of interest. The seismic sources near the area are identified first to quantify the seismic effect. Then, in this study, the background source zone (BSZ) is introduced to estimate the parameters of the Gutenberg-Richter (G-R) recurrence law. The law prescribes the relationship between the magnitude and the recurrence rate of the earthquake. Assuming an earthquake with the recurrence rate occurs, the ground motion prediction equation (GMPE) and the parameters in GMPE expressing the attenuated response to certain locations are introduced. Finally, the failure probability of the structure in the area is calculated by considering the probabilistic seismic capacity and the estimated response of the structure.

Although the socio-economic resilience index cannot solely determine the priority of decision-making, it can support considering the local circumstance regarding social, economic, institutional, and physical resilience to seismic risk. In the decision-making process, the socio-economic resilience index can provide information about each local government's relative level of socio-economic resilience which should be considered for deducting feasible decision-making. Moreover, though the initial priority of retrofit of roads is determined by quantitative factors such as the direct and indirect impact of seismic risk and the budget required for seismic retrofit, it is necessary to reflect qualitative factors such as regional risk, vulnerability, and recovery capabilities based on socio-economic resilience to the local government's final decision-making in decision-making module.

The resilience assessment of a complex road network, which is difficult to perform with existing sampling technology, can be calculated using the ANN-based Surrogate model, and the reliability of decision-making was improved. In addition, the software developed in this study can support decision-makers in making intuitive decisions by providing visual and graphical results of seismic performance evaluation, so that economical and reasonable seismic performance management can be achieved.

## Acknowledgments

This research was supported by a grant (21SCIP-B146946-04) from Smart Civil Infrastructure Research Program funded by Ministry of Land, Infrastructure and Transport of Korean government. The authors also would like to appreciate the contributions of Kwon Oh-Sung, Jong-Han Lee, Seong-Hoon Jeong, Jong-Keol Song, Jinsup Kim, Byung Ho Choi and Seungjun

Kim to finalize this paper. The author Junho Song appreciates the support by the Institute of Construction and Environmental Engineering at Seoul National University.

## ORCID

Dongjoo Kim  <http://orcid.org/0000-0001-8758-0906>

Junho Song  <https://orcid.org/0000-0003-4205-1829>

Young-Joo Lee  <http://orcid.org/0000-0003-3432-1411>

Sungsik Yoon  <http://orcid.org/0000-0002-0963-5278>

Dong Keun Yoon  <http://orcid.org/0000-0002-1573-5769>

Youngjun Kwon  <http://orcid.org/0009-0009-1486-3951>

Dongkyu Lee  <http://orcid.org/0000-0001-7155-9117>

Yeon-Woo Choi  <http://orcid.org/0000-0003-2805-0029>

## References

- Abrahamson NA, Youngs RR (1992) A stable algorithm for regression analyses using the random effects model. *Bulletin of the Seismological Society of America* 82(1):505-510, DOI: 10.1785/BSSA0820010505
- Akin O, Sahin M (2017) Active neuro-adaptive vibration suppression of a smart beam. *Smart Structures and Systems* 20(6):657-668, DOI: 10.12989/sss.2017.20.6.657
- Aomar RA (2010) A combined ahp-entropy method for deriving subjective and objective criteria weights. *International Journal of Industrial Eng.: Theory, Applications and Practice* 17(1):17-24, DOI: 10.23055/ijietap.2010.17.1.330
- Baker JW (2008) An introduction to probabilistic seismic hazard analysis (PSHA). *White Paper*, version 1:72
- Banerjee S, Vishwanath BS, Devendiran DK (2019) Multihazard resilience of highway bridges and bridge networks: A review. *Structure and Infrastructure Engineering* 15(12):1694-1714
- Boost (2008) The Boost Graph Library. [https://www.boost.org/doc/libs/1\\_37\\_0/libs/graph/doc/index.html](https://www.boost.org/doc/libs/1_37_0/libs/graph/doc/index.html)
- Chen M, Mangalathu S, Jeon JS (2022) Machine learning-based seismic reliability assessment of bridge networks. *Journal of Structural Engineering* 148(7):06022002
- Chen M, Mangalathu S, Jeon JS (2023) Betweenness centrality-based seismic risk management for bridge transportation networks. *Engineering Structures* 289:116301
- Cornell CA (1968) Engineering seismic risk analysis. *Bulletin of the Seismological Society of America* 58(5):1583-1606, DOI: 10.1785/BSSA0580051583
- Cornell CA, Banon H, Shakal AF (1979) Seismic motion and response prediction alternatives. *Earthquake Engineering & Structural Dynamics* 7(4):295-315, DOI: 10.1002/eqe.4290070402
- Du L, Peeta S (2014) A stochastic optimization model to reduce expected post-disaster response time through pre-disaster investment decisions. *Networks and Spatial Economics* 14(2):271-295, DOI: 10.1007/s11067-013-9219-1
- FEMA (2003) Multi-hazard loss estimation methodology earthquake model. Department of Homeland Security, Emergency Preparedness and Response
- FHWA (Federal Highway Administration) (2006) Seismic retrofitting manual for highway structures. No. FHWA-HRT-06-032, Federal Highway Administration, Washington, DC
- Gleich D (2008) MATLAB BGL, MATLAB Central. 2008, <https://kr.mathworks.com/matlabcentral/fileexchange/10922-matlabagl>
- Goda K, Hong H-P (2008) Spatial correlation of peak ground motions

- and response spectra. *Bulletin of the Seismological Society of America* 98(1):354-365, DOI: [10.1785/0120070078](https://doi.org/10.1785/0120070078)
- Gutenberg B, Richter CF (1944) Frequency of earthquakes in California. *Bulletin of the Seismological Society of America* 34(4):185-188, DOI: [10.1785/BSSA0340040185](https://doi.org/10.1785/BSSA0340040185)
- Joyner WB, Boore DM (1993) Methods for regression analysis of strong-motion data. *Bulletin of the Seismological Society of America* 83(2):469-487, DOI: [10.1785/BSSA0830020469](https://doi.org/10.1785/BSSA0830020469)
- Korea Authority of Land & Infrastructure Safety (KALIS) (2011) Guide line for seismic performance evaluation and improvement of existing facilities. No 11-B552016-000009-01, Korea Authority of Land & Infrastructure Safety, Korea
- Kang WH, Song J, Gardoni P (2008) Matrix-based system reliability method and applications to bridge networks. *Reliability Engineering & System Safety* 93(11):1584-1593
- Kramer SL (1996) Geotechnical earthquake engineering. Pearson Education India
- Lee SH, Kang JE, Bae HJ, Yoon DK (2015) Vulnerability assessment of the air pollution using entropy weights: Focused on ozone. *Journal of the Korean Association of Regional Geographers* 21(4):751-763
- Lee D, Song J (2021) Multi-scale seismic reliability assessment of networks by centrality-based selective recursive decomposition algorithm. *Earthquake Engineering & Structural Dynamics* 50(8):2174-2194, DOI: [10.1002/eqe.3447](https://doi.org/10.1002/eqe.3447)
- Lee D, Song J (2023) Risk-informed operation and maintenance of complex lifeline systems using parallelized multi-agent deep Q-network. *Reliability Engineering & System Safety* 239:109512, DOI: [10.1016/j.res.2023.109512](https://doi.org/10.1016/j.res.2023.109512)
- Lim HW, Song J (2012) Efficient risk assessment of lifeline networks under spatially correlated ground motions using selective recursive decomposition algorithm. *Earthquake Engineering & Structural Dynamics* 41(13):1861-1882, DOI: [10.1002/eqe.2162](https://doi.org/10.1002/eqe.2162)
- Mackie K, Stojadinovic B (2006) Post-earthquake functionality of highway overpass bridges. *Earthquake Engineering and Structural Dynamics* 35(1):77-93, DOI: [10.1002/eqe.534](https://doi.org/10.1002/eqe.534)
- Nguyen DH, Bui TT, De Roeck G, Wahab MA (2019) Damage detection in Ca-Non Bridge using transmissibility and artificial neural networks. *Structural Engineering and Mechanics* 71(2):175-183, DOI: [10.12989/sem.2019.71.2.175](https://doi.org/10.12989/sem.2019.71.2.175)
- Nyimbili PH, Erden T (2020) A hybrid approach integrating Entropy-AHP and GIS for suitability assessment of urban emergency facilities. *ISPRS International Journal of Geo-Information* 9(7):419, DOI: [10.3390/ijgi9070419](https://doi.org/10.3390/ijgi9070419)
- NYS DOT (New York State Department of Transportation) (2004) Bridge Safety Assurance Seismic Vulnerability Manual, New York State Department of Transportation, NY
- Onat O, Gul M (2018) Application of artificial neural networks to the prediction of out-of-plane response of infill walls subjected to shake table. *Smart Structures and Systems* 21(4):521-535, DOI: [10.12989/sss.2018.21.4.521](https://doi.org/10.12989/sss.2018.21.4.521)
- Rizzo P, Lanza di Scalea F (2006) Wavelet-based feature extraction for automatic defect classification in strands by ultrasonic structural monitoring. *Smart Structures and Systems* 2(3):253-274, DOI: [10.12989/sss.2006.2.3.253](https://doi.org/10.12989/sss.2006.2.3.253)
- Saaty RW (1987) The analytic hierarchy process—what it is and how it is used. *Mathematical Modelling* 9(3-5):161-176, DOI: [10.1016/0270-0255\(87\)90473-8](https://doi.org/10.1016/0270-0255(87)90473-8)
- Seo H, Kim J, Kim B (2022) Machine-learning-based surface ground-motion prediction models for South Korea with low-to-moderate seismicity. *Bulletin of the Seismological Society of America* 112(3):1549-64, DOI: [10.1785/0120210244](https://doi.org/10.1785/0120210244)
- Sextos AG, Kilanitis I, Kyriakou K, Kappos AJ (2017) Resilience of road networks to earthquakes. 16th World Conference on Earthquake Engineering
- Sianko I, Ozdemir Z, Khoshkholghi S, Garcia R, Hajirasouliha I, Yazgan U, Pilakoutas K (2020) A practical probabilistic earthquake hazard analysis tool: Case study Marmara region. *Bulletin of Earthquake Engineering* 18:2523-2555
- Sohn J, Kim TJ, Hewings GJ, Lee JS, Jang SG (2003) Retrofit priority of transport network links under an earthquake. *Journal of Urban Planning and Development* 129(4):195-210, DOI: [10.1061/\(ASCE\)0733-9488\(2003\)129:4\(195\)](https://doi.org/10.1061/(ASCE)0733-9488(2003)129:4(195))
- Sokolov V, Wenzel F, Jean W-Y, Wen K-L (2010) Un-certainty and spatial correlation of earthquake ground motion in Taiwan, *Terrestrial, Atmospheric and Oceanic Sciences* 21(6):905-921
- Tak H-Y, Suh W, Lee Y-J (2019) System-level seismic risk assessment of bridge transportation networks employing probabilistic seismic hazard analysis. *Mathematical Problems in Engineering*, DOI: [10.1155/2019/6503616](https://doi.org/10.1155/2019/6503616)
- Yoon S, Kim J, Kim M, Tak H-Y, Lee Y-J (2020) Accelerated system-level seismic risk assessment of bridge transportation networks through artificial neural network-based surrogate model. *Applied Sciences* 10(18):6476, DOI: [10.3390/app10186476](https://doi.org/10.3390/app10186476)
- Yoon S, Suh W, Lee Y-J (2021) Optimal decision making in post-hazard bridge recovery strategies for transportation networks after seismic events. *Geomatics, Natural Hazards and Risk* 12(1):2629-2653, DOI: [10.1080/19475705.2021.1961881](https://doi.org/10.1080/19475705.2021.1961881)
- Zardari NH, Ahmed K, Shirazi SM, Yusop ZB (2015) Weighting methods and their effects on multi-criteria decision making model outcome in water resources management. USA: Springer Press, DOI: [10.1007/978-3-319-12586-2](https://doi.org/10.1007/978-3-319-12586-2)